SSRG International Journal of Mechanical Engineering
ISSN: 2348-8360/ https://doi.org/10.14445/23488360/IJME-V11I4P104

Volume 11 Issue 4, 30-39, April 2024

Original Article

Computational Fluid Dynamic Analysis of Missile at Various Mach Numbers

V. Raghavender[1], S. V. Ramana[2], A. Krishnaiah[3]

[1,3]*Mechanical Engineering, University College of Engineering, Osmania University, Hyderabad, India.*
[2]*Mechanical Engineering, Vasavi College of Engineering, Hyderabad, India.*

[1]*Corresponding Author : vadla.raghav@gmail.com*

Received: 05 February 2024 Revised: 23 March 2024 Accepted: 13 April 2024 Published: 30 April 2024

Abstract *- The study conducted using Computational Fluid Dynamics (CFD), a missile serves several important objectives that contribute to the design, performance evaluation, and optimization of the missile. CFD simulations help assess the missile's aerodynamic behavior in various flight conditions. This includes analyzing lift, drag, and stability characteristics, which are crucial for achieving accurate trajectory predictions and target accuracy. By analyzing the flow patterns around the missile's surface, it can identify areas of high drag. Engineers can then modify the missile's geometry to reduce drag, resulting in improved fuel efficiency, longer range, and better maneuverability. The simulations enable the examination of how the missile's control surfaces affect its stability and maneuverability. This information is crucial for ensuring the missile can accurately follow its intended trajectory and perform any necessary mid-flight adjustments. Understanding the aerodynamic forces and thermal loads on the missile's structure helps assess its structural integrity. It can predict potential failure points and guide structural design improvements. Overall, the analysis of missiles plays a pivotal role in ensuring their effectiveness, accuracy, and safety. It helps engineers to understand complex fluid dynamics phenomena and their interactions with missile components, guiding the design process toward optimal solutions.*

Keywords *- Missile Aerodynamics, Lift, Drag, Stability.*

1. Introduction

In any flying body, four core forces help define the properties of its flight. Thrust and drag are opposing forces acting in the axial direction of the aircraft, while Lift and Weight are opposing forces acting transversely on the body [1]. Ideally it is required from an aircraft to have low drag and weight and more lift and thrust. This is the basic principle on which most air vehicles are designed, optimized and developed. A good aircraft will have a high lift-to-drag ratio to provide ample maneuverability [2]. There are many more complex analyses and variables that are also considered when designing any part of an aircraft. However, it all comes to these four fundamental forces in the end [3].

Missiles are an integral part of fighter aircraft armament, enhancing their combat capabilities and versatility. Fighters are equipped with a variety of missiles to engage targets both in the air and on the ground. These are sophisticated aerospace systems designed for various purposes, including defence, reconnaissance, and scientific research. Their success relies heavily on their aerodynamic performance, stability, and control. CFD analysis offers a comprehensive and cost-effective means to study these crucial aspects before physical prototypes are built and tested. When aircraft fly at speeds equal to or greater than the speed of sound, shocks are generated. Shockwaves, simply put, are an accumulation of air particles densely around the surface of the aircraft. They result in a considerable rise in static pressure and a decrease in flow velocity. Shocks can lead to flow separation and can severely affect the performance of the aircraft if not taken into consideration [8]. The strength of the shocks is directly proportional to the speed of the aircraft. So at higher Mach speeds, there will be large amounts of aerodynamic loads acting on the aircraft. To withstand such conditions, supersonic and hypersonic flights are structurally reinforced as required by the mission profile.

Modern missile design relies heavily on Computational Fluid Dynamics (CFD), which allows researchers and engineers to model and comprehend the intricate aerodynamic and fluid dynamic behaviour of missiles during flight. By leveraging advanced numerical techniques, CFD analysis provides insights into how airflows interact with the missile's geometry, aiding in the optimization of performance, stability, and overall effectiveness [5]. A finned missile is a type of guided projectile designed with aerodynamic fins [6] or control surfaces attached to its body. These fins play a critical role in stabilizing and controlling the missile's flight by generating aerodynamic forces that influence its trajectory and orientation [14].

2. Design and Methodology

A typical finned storage system with a leading edge sweep angle was part of the configuration. The software known as ICEM CFX post processor was utilised to generate the temperature, pressure, and velocity data.

Using the acquired results at the angle of attacks 0, 2, 6, pressure and flow visualisation data will be created in the software CFX. The test was conducted under standard Reynolds number circumstances of 2.4 × 106/ft, with mach numbers of 0.95 and 1.2 [21].

2.1. Test Article

A typical shop with four fins is included in the test piece. The fin design incorporates the leading edge sweep angle of the NACA 0008 airfoil section is 60 degrees. Applying a post-processor, it is possible to obtain all of the variations in pressure, temperature, and velocity at each location across the wing's surface.

2.2. Test Conditions

At a fixed Reynolds number per unit of 2.4 × 106/ft, data will be acquired at mach numbers of 0.95 and 1.2. The experiments will be carried out in two distinct ways.

1. Missile with a Mach number of 0.95
2. Missile with a Mach number of 1.2

2.3. Geometry

2.3.1. Store

Length	:	6.667 Inch
Radius	:	3.028 inches at the leading edge of the store
Fin	:	3.208 inches at trailing edge of store
Airfoil Section	:	NACA 0008 60 degree of leading edge

2.4. Governing Equations

Navier-Stokes equations, which regulate all fluid motions regardless of turbulent nature, are the combination of momentum, continuity, and energy equations. For buoyancy-driven flows, however, all three equations need to be calculated simultaneously due to temperature-dependent density factors in the momentum equation.

The momentum and continuity equations can be solved separately from the energy equation whenever the fluid characteristics remain constant.

The following is the general form of the governing equations:

Continuity equation

$$\frac{\partial}{\partial x_i}(\rho\tilde{u}_i) = 0 \tag{1}$$

Momentum equation

$$\rho\left[\frac{\partial\tilde{u}_i}{\partial t} + \frac{\partial\tilde{u}_i\tilde{u}_j}{\partial x_j}\right] = -\frac{\partial\tilde{p}}{\partial x_i} + \frac{\partial}{\partial x_j}\left(\mu\frac{\partial\tilde{u}_i}{\partial x_j}\right) + \rho g\beta\left(T_{ref} - \tilde{t}\right) \tag{2}$$

Energy equation:

$$\rho\left[\frac{\partial C_p\tilde{t}}{\partial t} + \frac{\partial C_p\tilde{u}_i\tilde{t}}{\partial x_j}\right] = \frac{\partial}{\partial x_j}\left(k\frac{\partial\tilde{t}}{\partial x_j}\right) + \tilde{S}_t \tag{3}$$

This process is known as Reynolds decomposition. The instantaneous quantity can be expressed as follows: where is the variable portion and is the time-averaged value. The aforementioned connection is substituted to yield the Navier-Stokes Averaged Reynolds (RANS) equations. There are several forms of the RANS:

$$\frac{\partial}{\partial x_i}(\rho U_i) = 0 \tag{4}$$

$$\rho\left[\frac{\partial U_i}{\partial t} + \frac{\partial U_iU_j}{\partial x_j}\right] = -\frac{\partial P}{\partial x_i} + \frac{\partial}{\partial x_j}\left(\mu\frac{\partial U_i}{\partial x_j} - \rho\overline{u_iu_j}\right) + \rho g\beta\left(T_{ref} - T\right) \tag{5}$$

Where,

S_t is the source term. The unknowns $\rho\overline{u_iu_j}, \rho\overline{u_jt}$ are referred to as the velocity temperature correlation and Reynolds stress, respectively. Both two terms cause the entire RANS problem, which is also known as the Turbulence Closure Problem. We must model both terms in order to close the RANS equations.

2.5. Navier-Stokes Equations

2.5.1. Conservation of Mass

The mass shift in the CV and the net mass inflow and outflow through the control surfaces determine the unstable mass in the control volume.

$$\frac{\partial(\rho dxdydz)}{\partial t} + (\rho u + \frac{\partial\rho u}{\partial x}dx)dydz - \rho udydz + (\rho v + \frac{\partial\rho v}{\partial y}dy)dxdz - \rho vdxdz + (\rho w + \frac{\partial\rho w}{\partial z}dz)dxdy - \rho wdxdy = 0$$

or simplified

$$\frac{\partial\rho}{\partial t} + \frac{\partial\rho u}{\partial x} + \frac{\partial\rho v}{\partial y} + \frac{\partial\rho w}{\partial z} = 0.$$

2.5.2. Conservation of Momentum

$$\vec{F}_x = \frac{\partial\rho u}{\partial t}dxdydz + \frac{\partial\rho uu}{\partial x}dxdydz + \frac{\partial\rho vu}{\partial y}dxdydz + \frac{\partial\rho wu}{\partial z}dxdydz \tag{6}$$

$$\vec{F}_y = \frac{\partial \rho v}{\partial t} dxdydz + \frac{\partial \rho uv}{\partial x} dxdydz + \frac{\partial \rho vv}{\partial y} dxdydz + \frac{\partial \rho wv}{\partial z} dxdydz \quad (7)$$

$$\vec{F}_z = \frac{\partial \rho w}{\partial t} dxdydz + \frac{\partial \rho uw}{\partial x} dxdydz + \frac{\partial \rho vw}{\partial y} dxdydz + \frac{\partial \rho ww}{\partial z} dxdydz$$

or

$$\vec{F}_i = \frac{\partial \rho u_i}{\partial t} dxdydz + \frac{\partial \rho u_i u_j}{\partial x_j} dxdydz$$

Our shear equation for Newtonian fluids, when the rate of strain relationship is added, gives

$$\tau_{ij} = \mu e_{ij} + (\lambda \frac{\partial u_i}{\partial x_i} - p)\delta_{ij}$$

or

$$\tau_{ij} = \mu(\frac{\partial u_i}{\partial x_j} + \frac{\partial u_j}{\partial x_i}) + (\lambda \frac{\partial u_i}{\partial x_i} - p)\delta_{ij}$$

Where δij, the *Kronecker delta*, is

$$\delta_{ij} = \begin{matrix} 1 & if \;\; i = j \\ 0 & if \;\; i \neq j \end{matrix}$$

For a clear explanation of why the shear stress takes on this particular form, see Viscous Fluid Flow.

2.5.3. Energy Equation

$$\frac{\partial \rho e}{\partial t} + \frac{\partial \rho ue}{\partial x} + \frac{\partial \rho ve}{\partial y} + \frac{\partial \rho we}{\partial z} = -\frac{\partial q_x}{\partial x} - \frac{\partial q_y}{\partial y} - \frac{\partial q_z}{\partial z} + \frac{\partial \dot{w}_x}{\partial x} + \frac{\partial \dot{w}_y}{\partial y} + \frac{\partial \dot{w}_z}{\partial z}$$

$$\frac{\partial \rho e}{\partial t} + \frac{\partial \rho u_i e}{\partial x_i} = \frac{\partial}{\partial x_i} k \frac{\partial T}{\partial x_i} + \frac{\partial \tau_{ij} u_j}{\partial x_i} \quad (8)$$

The thermal energy equation is one of the most used versions of the energy equation; it removes mechanical energy and leaves thermal energy by subtracting the momentum equation from the total energy equation.

$$e = \tilde{u} + \frac{V^2}{2}$$

$$\frac{\partial \rho h}{\partial t} + \frac{\partial \rho u_i h}{\partial x_i} = \frac{\partial}{\partial x_i} k \frac{\partial T}{\partial x_i} + \tau_{ij} \frac{\partial u_j}{\partial x_i}$$

2.6. Turbulence Modelling

The Reynolds stress and temperature velocity correlation terms in the RANS equations are closed by Boussinesq approximation.

$$\rho \left[\frac{\partial C_p T}{\partial t} + \frac{\partial C_p U_i T}{\partial x_j}\right] = \frac{\partial}{\partial x_j}\left(k \frac{\partial T}{\partial x_j} - \rho \overline{u_j t}\right) + \tilde{S}_t$$

$$-\rho \overline{u_i u_j} = \mu_t \left(\frac{\partial U_i}{\partial x_j} + \frac{\partial U_j}{\partial x_i}\right) - \frac{2}{3}\delta_{ij}\rho k \quad (9)$$

The turbulent heat flux

$$-\rho \overline{u_j t} = \frac{\mu_t}{Pr_t} \frac{\partial T}{\partial x_j}$$

Where Pr_t is Turbulent Prandtl number

δ_{ij} is kronecker delta

μ_t is turbulent viscosity

Unlike normal viscosity, turbulent viscosity depends upon the nature of flow behaviour. The turbulent viscosity is the property of the flow but not of the fluid.

After these approximations, the resulting governing equations are:

$$\frac{\partial}{\partial x_i}(\rho U_i) = 0$$

$$\rho \left[\frac{\partial U_i}{\partial t} + \frac{\partial U_i U_j}{\partial x_j}\right] = -\frac{\partial P}{\partial x_i} + \frac{\partial}{\partial x_j}\left((\mu + \mu_t)\frac{\partial U_i}{\partial x_j}\right) + \rho g \beta (T_{ref} - T)$$

$$\rho \left[\frac{\partial C_p T}{\partial t} + \frac{\partial C_p U_i T}{\partial x_j}\right] = \frac{\partial}{\partial x_j}\left[\left(\frac{\mu}{Pr\frac{\mu_t}{Pr_t}} \bigcirc \frac{\partial T}{\partial x_j}\right)[]_t\right]$$

The only unknown term in the above equations is the turbulent viscosityμ_t, to get the values of turbulent viscosity, we solve for turbulence models.

$$a(E) = \frac{1}{v_e}\left[\frac{2X(E)}{\left(\phi^I(E) - \phi^{II}(E)\right) - X(E)\left(\phi^I(E) + \phi^{II}(E)\right)}\right] \quad (10)$$

3. Design

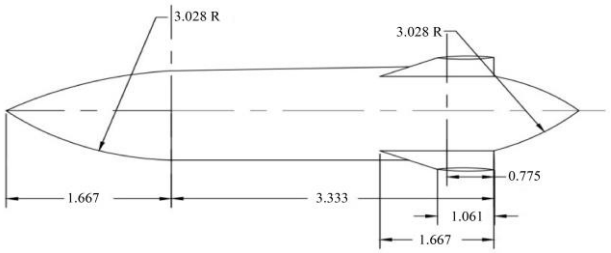

Fig. 1 Missile

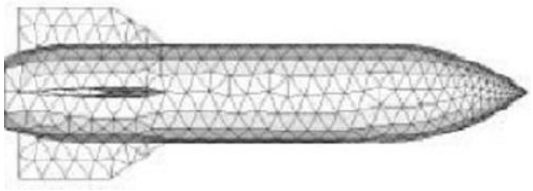

Fig. 2 Mesh

3.1. Mesh Parameters

Table 1. Mesh data

MESH	STORE	FIN
Global scale factor	**1**	**1**
Maximum Element	**32**	**8**
Initial height	**0**	**0**
Height ratio	**0**	**0**
No of Prism Layers	**0**	**0**
Total Height	**0**	**0**
Maximum Size	**15**	**3**

4. Results and Discussion

4.1. At M 0.95_D0_a0

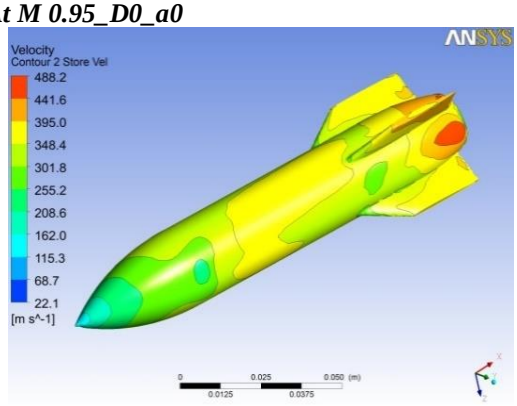

Fig. 3 Velocity contour at 0.95 mach at 0 aoa

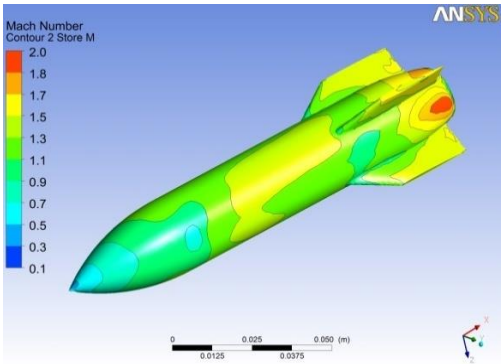

Fig. 4 Mach number contour at 0.95 mach at 0 aoa

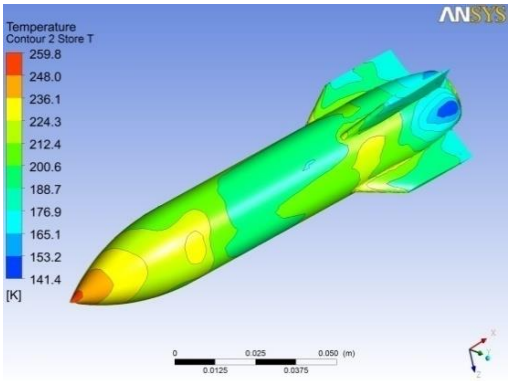

Fig. 5 Temperature contour at 0.95 mach at 0 aoa

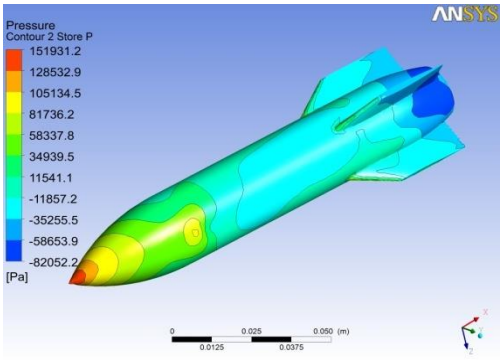

Fig. 6 Pressure contour at 0.95 mach at 0 aoa

4.2. At M 0.95_D0_a2

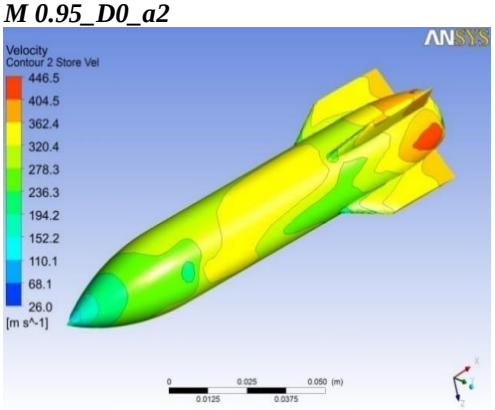

Fig. 7 Velocity contour at 0.95 mach at 2 aoa

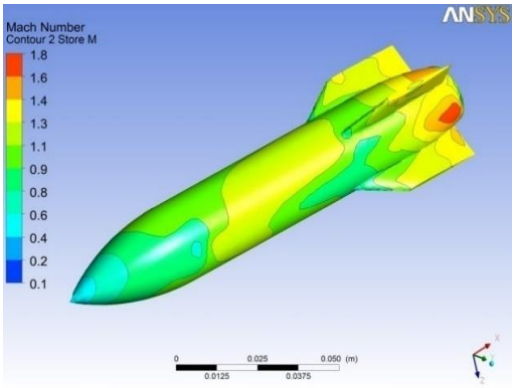

Fig. 8 Mach number contour at 0.95 mach at 2 aoa

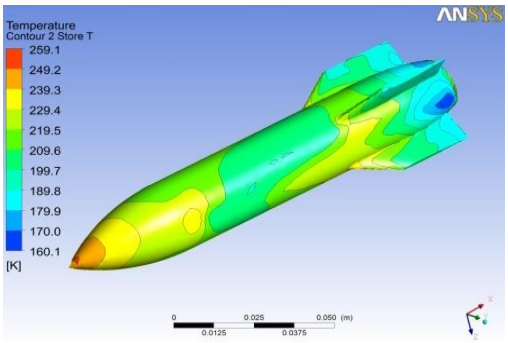

Fig. 9 Temperature contour at 0.95 mach at 2 aoa

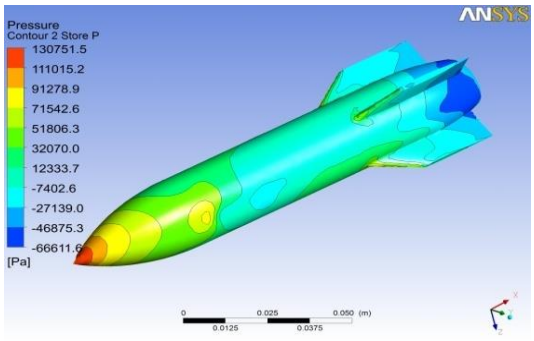

Fig. 10 Pressure contour at 0.95 mach at 2 aoa

4.3. At M 0.95_D0_a6

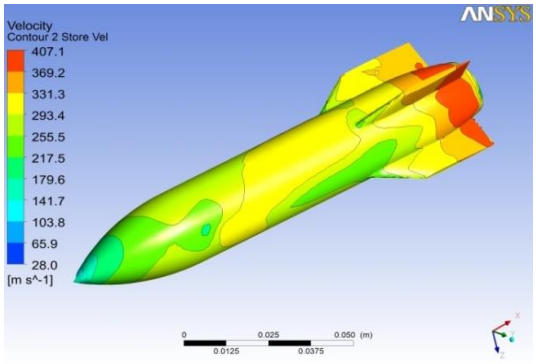

Fig. 11Velocity contour at 0.95 mach at 6 aoa

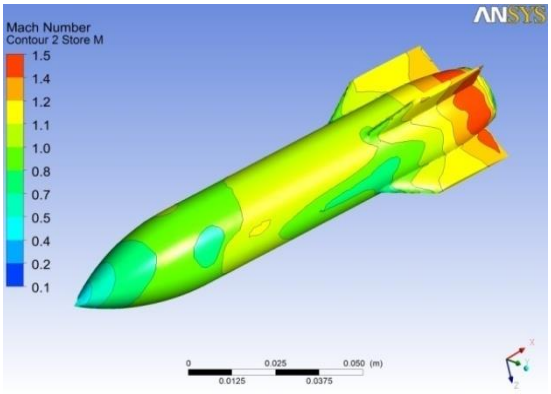

Fig. 12 Mach number contour at 0.95 mach at 6 aoa

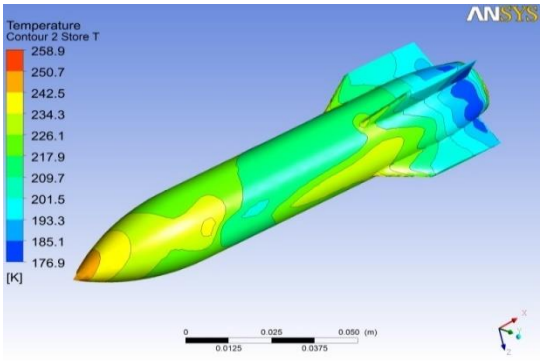

Fig. 13 Temperature contour at 0.95 mach at 6 aoa

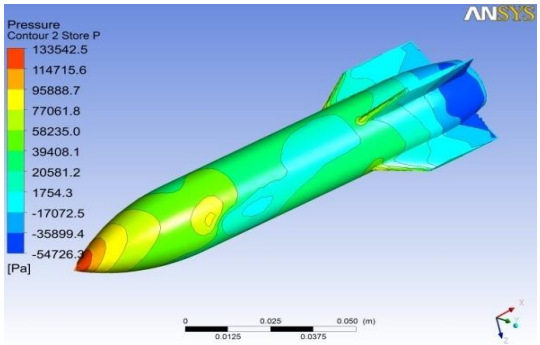

Fig. 14 Pressure contour at 0.95 mach at 6 aoa

4.4. At M 1.2_D0_a0

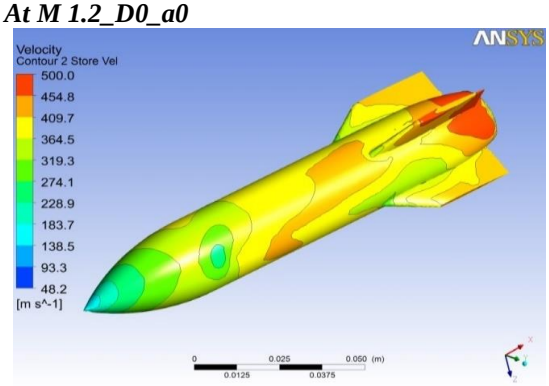

Fig. 15 Velocity contour at 1.2 mach at 0 aoa

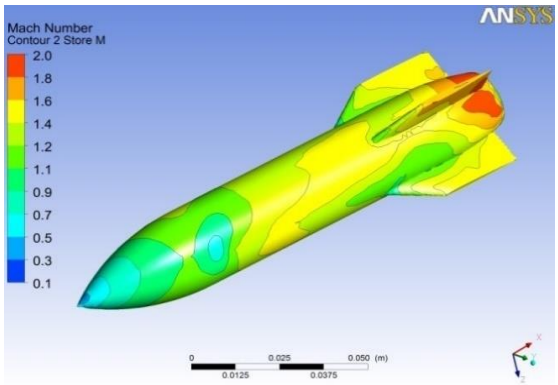

Fig. 16 Mach number contour at 1.2 mach at 0 aoa

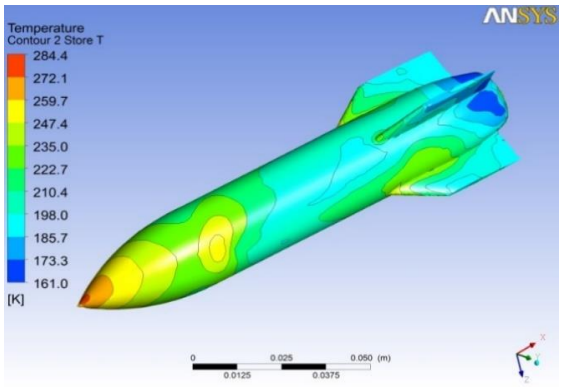

Fig. 17 Temperature contour at 1.2 mach at 0 aoa

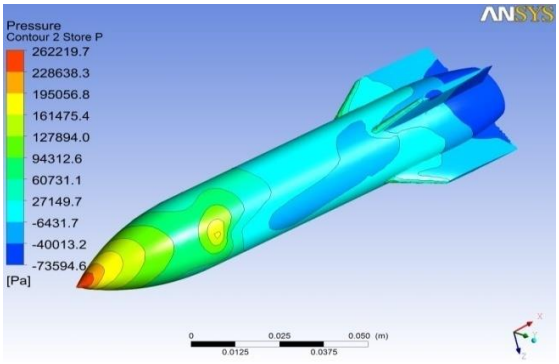

Fig. 18 Pressure contour at 1.2 mach at 0 aoa

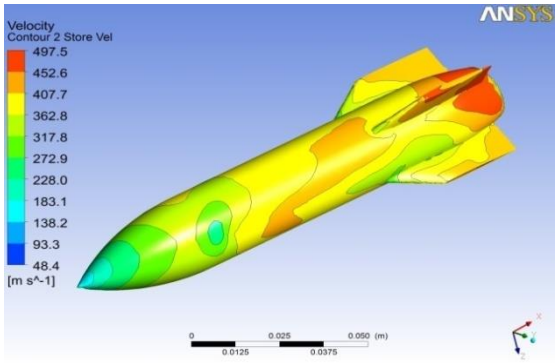

Fig. 22 Pressure contour at 1.2 mach at 2 aoa

4.5. At M 1.2_D0_a2

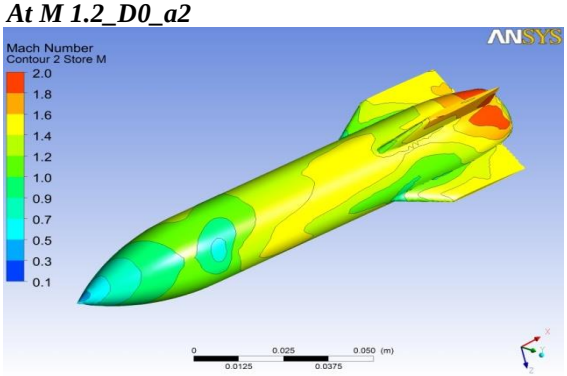

Fig. 19 Velocity contour at 1.2 mach at 2 aoa

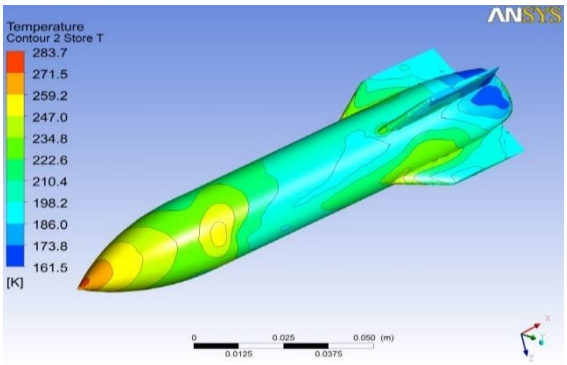

Fig. 20 Mach number contour at 1.2 mach at 2 aoa

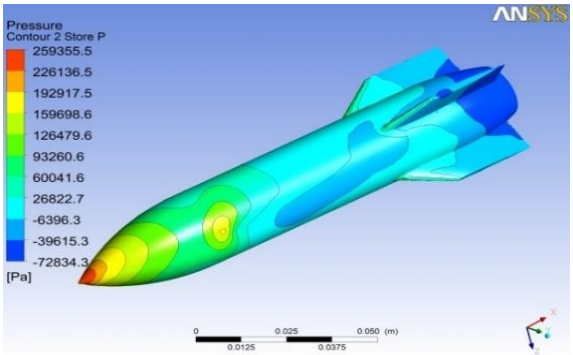

Fig. 21 Temperature contour at 1.2 mach at 2 aoa

4.6. At M 1.2_D0_a6

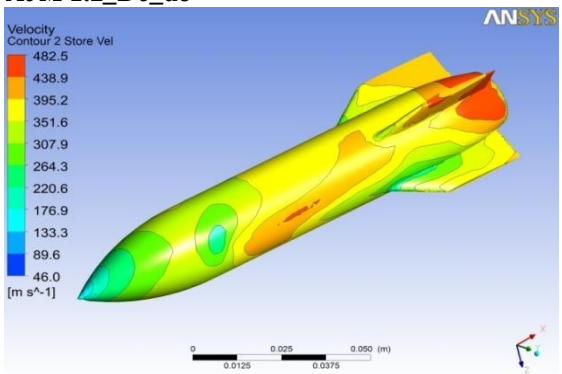

Fig. 23 Velocity contour at 1.2 mach at 6 aoa

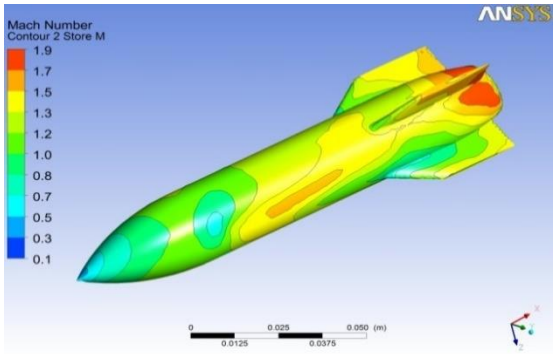

Fig. 24 Mach number contour at 1.2 mach at 6 aoa

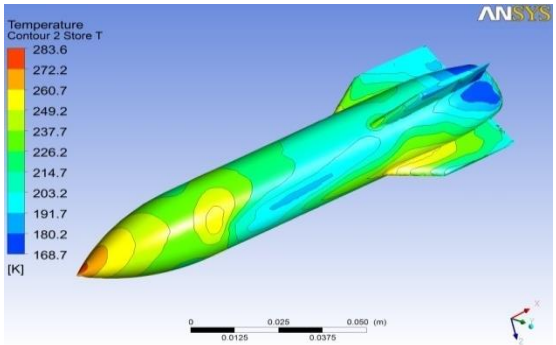

Fig. 25 Temperature contour at 1.2 mach at 6 aoa

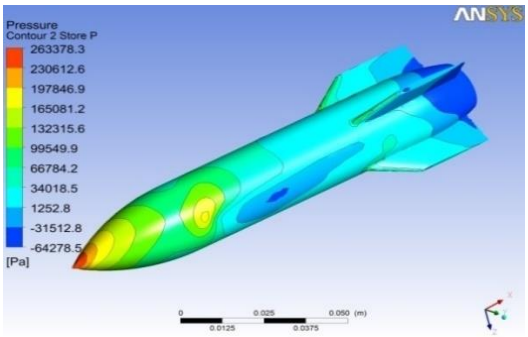

Fig. 26 Pressure contour at 1.2 mach at 6 aoa

4.7. Normal Force on Store

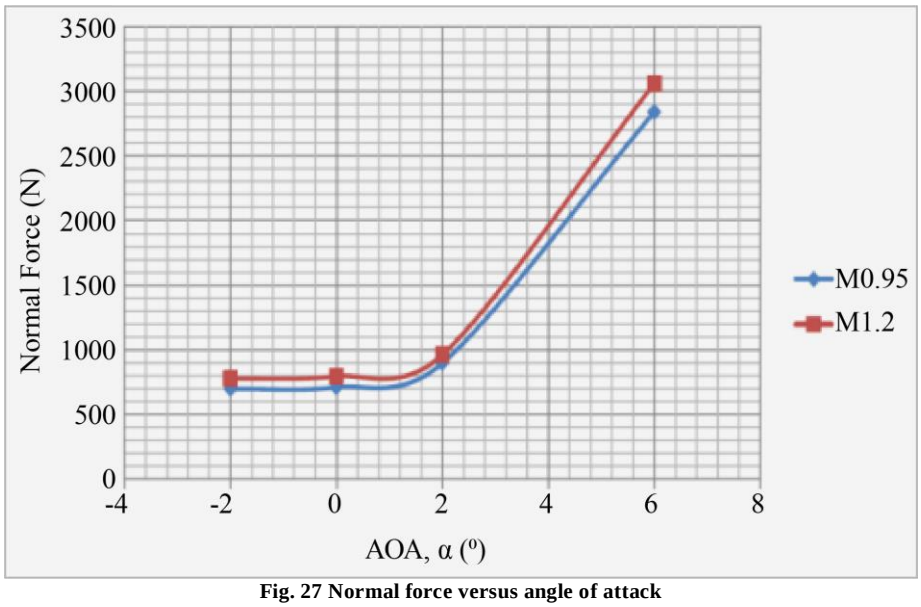

Fig. 27 Normal force versus angle of attack

4.8. Pitching Moment on Store

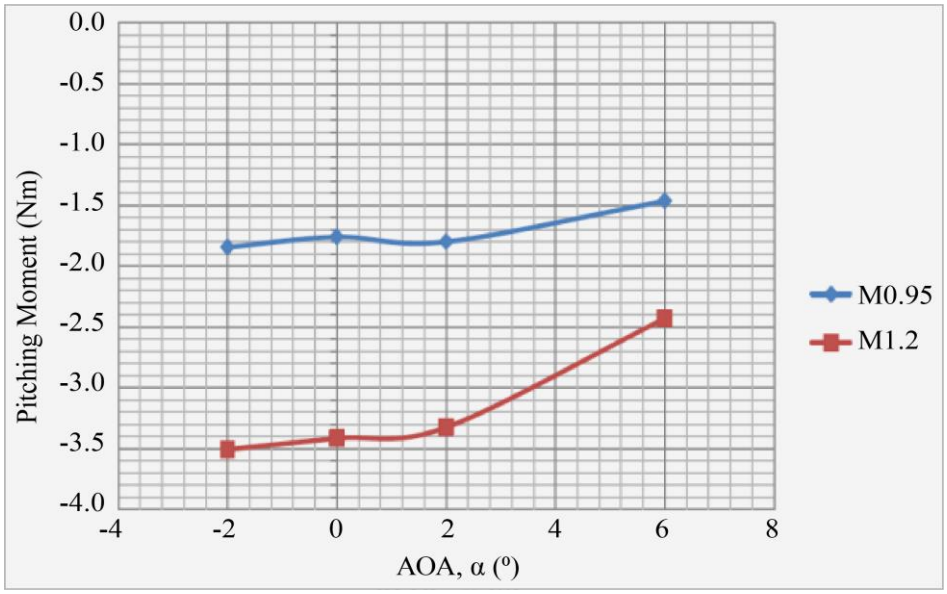

Fig. 28 Pitching moment versus angle of attack

4.9. Rolling Moment on Store

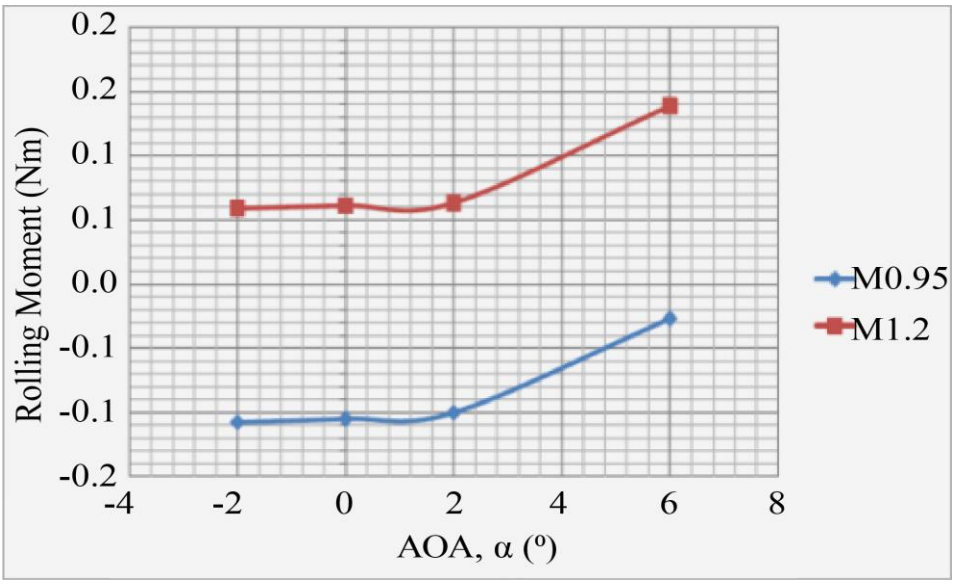

Fig. 29 Rolling moment versus angle of attack

4.10. Yawing Moment in Store

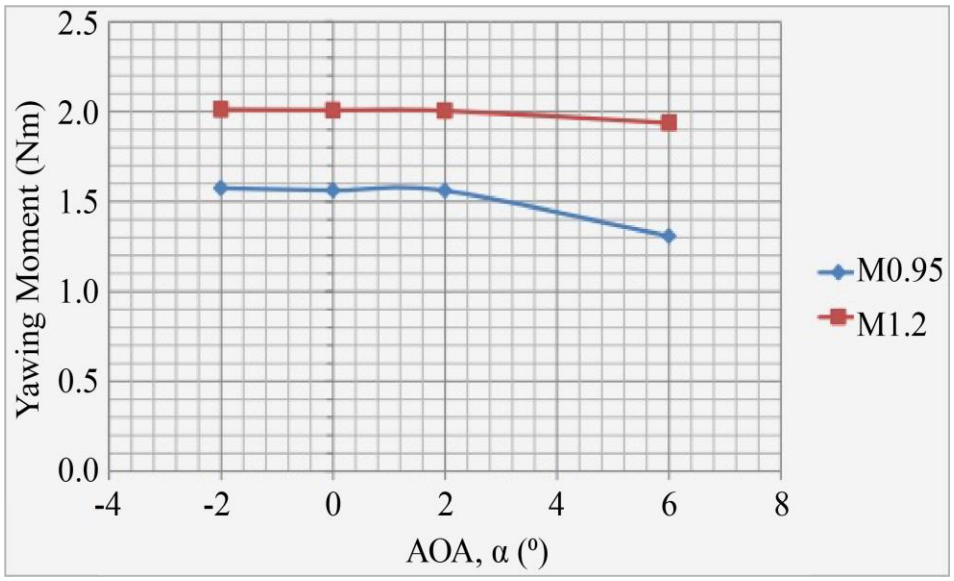

Fig. 30 Yawing moment versus angle of attack

Table 2. Comparison between M0.95 and M 1.25

Condition	M0.95d0a0	M0.95d0a2	M0.95d0a6	M1.2d0a0	M1.2d0a2	M1.2d0a6
Force_X	65.14	58.71	53.45	95.46	94.49	93.35
Force_Y	26.47	26.25	24.14	28.37	28.80	28.03
Force_Z	-32.44	-29.72	-7.42	1.07	2.56	34.69
Pitching_Moment	-2.33	-1.80	-1.46	-3.41	-3.32	-2.43
Rolling_Moment	-0.08	-0.10	-0.03	0.06	0.06	0.14
Yawing_Moment	1.80	1.56	1.31	2.01	2.00	1.94
AOA	0	2	6	0	2	6

5. Conclusion

In conclusion, the application of Computational Fluid Dynamics (CFD) analysis to missiles offers a transformative approach to designing, optimizing, and understanding their aerodynamic behavior and overall performance. This powerful computational tool has the potential to revolutionize missile design and testing by providing accurate insights into complex fluid dynamics phenomena that are crucial to their successful operation. Through this analysis, engineers and researchers gain a deep understanding of how air flows around a missile, its stability characteristics, heat distribution, and the forces it experiences during flight. These insights enable them to make informed design decisions that lead to enhanced accuracy, efficiency, and mission success.

The CFD analysis process involves meticulously preparing the missile's geometry, generating a suitable mesh, selecting appropriate physics models, and setting up boundary conditions. By choosing the right solver and executing simulations, a wealth of data is generated. Moreover, the iterative nature of CFD analysis encourages design refinement. In essence, CFD analysis revolutionizes missile design by providing a virtual laboratory to explore and understand the complex aerodynamic and fluid dynamics phenomena that affect missiles in flight. The insights gained from these simulations drive innovation, improve efficiency, and ultimately contribute to the creation of more effective and capable missile systems for a variety of applications, including defense, research, and exploration.

Conflicts of Interest

This section is compulsory. A competing interest exists when professional judgment concerning the validity of research is influenced by a secondary interest, such as financial gain. We require that our authors reveal any possible conflict of interest in their submitted manuscripts. If there is no conflict of interest, authors should state that "The author(s) declare(s) that there is no conflict of interest regarding the publication of this paper."

Acknowledgments

V Raghavender: Conceptualization, Methodology, Software, Validation, Writing – original draft, Writing – review and editing. Dr SV Ramana: Supervision, Writing – original draft, Writing – review and editing. Prof Krishnaiah Arkanti: Writing –review and editing.

References

[1] Bilal A. Bhutta, and Clark H. Lewis, "Supersonic/Hypersonic Flow Field Predictions over Typical Finned Missile Configurations," *Journal of Spacecraft and Rockets*, vol. 30, no. 6, pp. 674–681, 1993. [CrossRef] [Google Scholar] [Publisher Link]

[2] Hasan Taher M. Elkamel, Bambang Basuno, and Abobaker Mohammed Alakashi, "Two Dimensional Compressible Flow Analysis over a Generic Cruise Missile Model," *Applied Mechanics and Materials*, vol. 465–466, pp. 358–362, 2013. [CrossRef] [Google Scholar] [Publisher Link]

[3] Charles H. Murphy, and William H. Mermagen, "Flight Motion of a Continuously Elastic Finned Missile," *Journal of Guidance, Control, and Dynamics*, vol. 26, no. 1, pp. 89–98. 2003. [CrossRef] [Google Scholar] [Publisher Link]

[4] Payal Tembhurnikar et al., "Computational Analysis of Flow Field Over Missile Separated from Weapon Bay Cavity at Mach 2 and 5," *2021 IEEE Pune Section International Conference (PuneCon)*, Pune, India, pp. 1–6, 2021. [CrossRef] [Google Scholar] [Publisher Link]

[5] Kevin A. Wise, and David J.B. Roy, "Agile Missile Dynamics and Control," *Journal of Guidance, Control, and Dynamics*, vol. 21, no. 3, pp. 441–449, 1998. [CrossRef] [Google Scholar] [Publisher Link]

[6] M.J. Bamber, "Two Methods of Obtaining Aircraft Trajectories from Wind Tunnel Investigations," *AERO Report*, 1960. [Google Scholar]

[7] R. Meyer, A. Cenko, and S. Yaros, "An Influence Function Method for Predicting Store Aerodynamic Characteristics during Weapon Separation," *12th Navy Symposium on Aeroballistics*, 1981. [Google Scholar] [Publisher Link]

[8] Abdollah Arabshahi, and David Whitfield, "A Multi-Block Approach to Solving the Three-Dimensional Unsteady Euler Equations About a Wing-Pylon-Store Configuration," *16th Atmospheric Flight Mechanics Conference*, 1989. [CrossRef] [Publisher Link]

[9] K. Keen, "New Approaches to Computational Aircraft/Store Weapons Integration," *28th Aerospace Sciences Meeting*, 1990. [CrossRef] [Google Scholar] [Publisher Link]

[10] Lawrence E. Lijewski, "Transonic Euler Solutions on Mutually Interfering Finned Bodies," *AIAA Aeronautics, Astronautic Journal*, vol. 28, no. 6, pp. 982-988, 1990. [CrossRef] [Google Scholar] [Publisher Link]

[11] Lawrence E. Lijewski, and Norman E. Suhs, "Time-Accurate Computational Fluid Dynamics Approach to Transonic Store Separation Trajectory Prediction," *Journal of Aircraft*, vol. 31, no. 4, pp. 886-891, 1994. [CrossRef] [Google Scholar] [Publisher Link]

[12] Sun-Eun Kim et al., "A Reynolds - Averaged Navier-Stokes Solver Using Unstructured Mesh-Based Finite-Volume Scheme," *36th AIAA Aerospace Sciences Meeting and Exhibit*, 1998. [CrossRef] [Google Scholar] [Publisher Link]

[13] E. Loth, K. Kailasanath, and R. Lohner, "Supersonic Flow Over an Axisymmetric Backward -Facing Step," *Journal of Spacecraft and Rockets*, vol. 29, no. 3, pp. 352–359, 1992. [CrossRef] [Publisher Link]

[14] E. Rolland Heim, *CFD Wing/Pylon/Finned Store Mutual Interference Wind Tunnel Experiment*, Arnold Engineering Development Center, Air Force Systems Command, United States Air Force, USA, pp. 1-63, 1991. [Google Scholar] [Publisher Link]

[15] J.B. Carman, D.W. Hill, and J.P. Christopher, "Store Separation Testing Techniques at the Arnold Engineering Development Center," *Volume II: Description of Captive Trajectory Store Separation Testing in the Aerodynamic Wind Tunnel (4T)*, USA, pp. 1-133, 1980. [Google Scholar] [Publisher Link]

[16] R.J. Arnold, and C.S. Epstein, *AGARD Flight Test Techniques Series, Volume 5 on Store Separation Flight Testing*, AGARD, pp. 1-146, 1986. [Google Scholar] [Publisher Link]

[17] Mohamed Yousuf et al., "Demonstration of Automated CFD Process Using Meshless Technology," *Proceedings of the 6th European Conference on Computational Fluid Dynamics*, pp. 1-18, 2014. [Google Scholar] [Publisher Link]

[18] Saurabh Pandey, and Bharat R. Agrawal, "Store Separation Simulation Using Oct-tree Grid Based Solver," *4th Symposium on Applied Aerodynamics and Design of Aerospace Vehicles*, pp. 1-10, 2009. [Google Scholar] [Publisher Link]

[19] Scott Murman, Michael Aftosmis, and Marsha Berger, "Simulations of 6-DOF Motion with a Cartesian Method," *AIAA Paper, 41st Aerospace Sciences Meeting and Exhibit*, 2003. [CrossRef] [Google Scholar] [Publisher Link]

[20] P. Thorigny, D. Bailly, and P. Denis, "Store Separation Trajectory Simulations using "MISSILE" Onera Semi-empirical Aero-Prediction Code," *4th European Conference For Aerospace Science, EUCASS*, Saint Petersburg, Russia, 2011. [Google Scholar]

[21] V. Raghavender, and R. Kannan, "Computational Aerodynamic Analysis on Store Separation from Aircraft Using Pylon," *International Journal of Engineering Science Invention*, pp. 27-31, 2014. [Publisher Link]